RESEARCH ARTICLE | JANUARY 22 2024

Nanoscopic spin-wave channeling along programmable magnetic domain walls in a CoFeB/$BaTiO_3$ multiferroic heterostructure

Weijia Zhu ; Huajun Qin ; Sebastiaan van Dijken

Appl. Phys. Lett. 124, 042401 (2024)
https://doi.org/10.1063/5.0179748

Applied Physics Letters ARTICLE pubs.aip.org/aip/apl

Nanoscopic spin-wave channeling along programmable magnetic domain walls in a $CoFeB/BaTiO_3$ multiferroic heterostructure

Cite as: Appl. Phys. Lett. **124**, 042401 (2024); doi: 10.1063/5.0179748
Submitted: 4 October 2023 · Accepted: 2 January 2024 ·
Published Online: 22 January 2024

Weijia Zhu,[1] Huajun Qin,[2,3,a)] and Sebastiaan van Dijken[1,a)]

AFFILIATIONS

[1]NanoSpin, Department of Applied Physics, Aalto University School of Science, P.O. Box 15100, FI-00076 Aalto, Finland
[2]School of Physics and Technology, Wuhan University, Wuhan 430072, China
[3]Wuhan Institute of Quantum Technology, Wuhan 430206, China

[a)]**Authors to whom correspondence should be addressed:** qinhuajun@whu.edu.cn and sebastiaan.van.dijken@aalto.fi

ABSTRACT

We report a micromagnetic study on spin-wave propagation along magnetic domain walls in a ferromagnetic/ferroelectric bilayer. In our system, strain coupling between the two ferroic materials and inverse magnetostriction produce a fully correlated domain pattern wherein straight and narrow ferroelectric domain walls pin the magnetic domain walls. Consequently, an external magnetic field does tailor the spin structure of the magnetic domain walls instead of moving them. We use experimental parameters from a previously studied $CoFeB/BaTiO_3$ material system to investigate the potential of artificial multiferroics for programmable nanoscopic spin-wave channeling. We show that spin waves are transported along the pinned magnetic domain walls at zero magnetic field and low frequency due to a local demagnetizing field. Further, switching of the domain wall spin structure from a head-to-tail to a head-to-head configuration abruptly changes the propagating spin-wave mode. We study the effect of magnetic field strength on the localized modes and discuss reversible control of spin-wave channeling via electric-field-driven magnetic domain wall motion. Nanoscopic guiding of propagating spin waves by an electric field, in combination with positional robustness to and mode programming by an external magnetic field, offers prospects for low-power and reconfigurable domain-wall-based magnonic devices.

Magnonics is an emerging technology that utilizes spin waves for energy efficient wave-based logic and unconventional computing in reconfigurable circuits.[1–6] To become competitive, schemes for the channeling and manipulation of spin waves need to improve and the footprint of magnonic circuits must scale down. As a potential solution, nano-sized magnetic domain walls operating as reconfigurable spin-wave nanochannels have been proposed and demonstrated.[7–20] The chiral spin structure of magnetic domain walls localizes the transport of spin waves below the ferromagnetic resonance (FMR) frequency of the uniformly magnetized domains.[21] Experiments have shown that domain walls carrying spin waves with well-defined wave vectors can be repositioned by a magnetic field,[7] that spin waves with nanoscale wavelengths can be injected into magnetic domain walls using a vortex core or other anisotropic spin textures,[8,9] and that prototypical domain-wall circuits can be patterned by thermally assisted magnetic scanning probe lithography (tam-SPL).[10] In addition to these experimental breakthroughs, various effects and device concepts have been theorized and simulated, including unidirectional spin-wave channeling,[13–15,17] the propagation of spin waves along antiferromagnetic and synthetic antiferromagnetic domain walls,[18,19] and reconfigurable spin-wave couplers based on domain-wall channels.[20]

The manipulation of propagating spin waves in a magnetic domain wall is complicated by the fact that an externally applied magnetic field moves the wall in a magnetic film without significantly altering its spin structure. To control the position of domain-wall nanochannels, micrometer-sized rectangles with a Landau-like domain pattern[7,9] and tam-SPL[10] have been employed in experiments. Here, we assess spin-wave transport in magnetic domain walls that are pinned strongly onto ferroelectric domain walls in a strain-coupled ferromagnetic/ferroelectric bilayer. This artificial multiferroic system, which has been studied extensively,[22] offers attractive features for nanoscopic spin-wave channeling. First, the magnetic domain walls are straight and pinned by abrupt changes of magnetic anisotropy induced by strain transfer from ferroelastic stripe domains in the

ferroelectric layer. An external magnetic field does, therefore, not move the magnetic domain walls, but it alters their spin structure,[23] enabling programming of propagating spin-wave modes. Second, an applied electric field can move the magnetic domain walls by displacing the ferroelectric domain walls that pin them.[24,25] This feature holds the potential of rerouting spin-wave signals by voltages. Importantly, in the strain-coupled ferromagnetic/ferroelectric bilayer considered here, the manipulation of spin-wave modes and the positioning of nanochannels are separated fully, with one being controlled by a magnetic field and the other being driven by an electric field.

In previous studies, we already investigated the use of strain-coupled ferromagnetic/ferroelectric bilayers in magnonics. For instance, we showed that pinned magnetic domain walls can act as broadband spin-wave emitters,[26,27] we demonstrated programmable filtering of spin-wave transmission across such walls,[28] and we realized voltage control of spin-wave transport by ferroelectric domain wall motion.[29] Here, we focus on the propagation of spin waves along pinned magnetic domain walls. Figure 1(a) shows the configuration of our system. It consists of a ferroelectric layer with regular stripe domains exhibiting 90° rotations of the ferroelectric polarization. Strain transfer from the ferroelastic domains in the ferroelectric layer to an adjacent ferromagnetic film induces a fully correlated magnetic domain pattern.[24,30] The magnetic domains labeled a_1 and a_2 exhibit strain-induced uniaxial magnetic anisotropy with a 90° angle between the easy magnetization axes. Because of the abrupt rotation of magnetic anisotropy, the Néel-type magnetic domain wall is pinned strongly onto the ferroelectric domain wall. We simulate spin-wave propagation along this wall by exciting spin waves using an antenna structure that is oriented perpendicular to the wall.

The micromagnetic simulations are performed in MuMax3 software.[31] The input parameters are taken from experiments on a CoFeB/$BaTiO_3$ bilayer with fully correlated domains and pinned magnetic domain walls.[27] We consider a 25-nm-thick CoFeB film. The simulation area is $12.8 \times 6.4\ \mu m^2$, and it includes one a_1 and one a_2 domain, which are both 3.2 μm wide. The simulation area is discretized into $6.25 \times 6.25 \times 12.50\ nm^3$ cells. Periodic boundary conditions are applied along the x and y directions to mimic a sample with alternating a_1 and a_2 domains, as observed in experiments. The domains are separated by a pinned magnetic domain wall acting as a spin-wave nanochannel. The strength of uniaxial magnetic anisotropy in the two domains is set to $K_u = 5 \times 10^4\ J/m^3$, and its easy axis rotates abruptly by 90° between domains. The saturation magnetization, Gilbert damping constant, and the exchange constant of the CoFeB film are set to $M_s = 1150$ kA/m, $\alpha = 0.005$, and $A_{ex} = 21$ pJ/m. We use an in-plane magnetic field to initialize two types of magnetic domain walls, narrow walls in which the magnetization aligns in a head-to-tail configuration and much broader walls with a head-to-head spin structure.[23,28] Spin waves are excited by an out-of-plane sinusoidal ac magnetic field applied over a 50-nm-wide area acting as the microwave antenna [Fig. 1(a)]. The ac excitation field is set to 10 mT. An external magnetic bias field is applied perpendicular to the domain wall in some simulations. Snapshots of spin-wave maps and line profiles representing steady-state dynamics are taken after 50 ns.

Figure 1(b) presents the spatial distribution of magnetization in the a_1 and a_2 domains at zero magnetic field after initialization by an external magnetic field along the positive y direction. In this remanent state, the magnetization aligns at an angle of 45° and 135° with respect to the x axis within the two domains. The thus-formed head-to-tail magnetic domain wall is narrow, and its magnetization is oriented along the y axis in the center of the wall. Because of a large demagnetizing field [Fig. 1(c)], this magnetic domain wall can act as a nanochannel for the transport of spin waves. Figure 1(d) shows the spatial distribution of magnetization in the a_1 and a_2 domains at zero magnetic field after initialization by an external magnetic field along the negative x direction. Now, the remanent state comprises a pinned magnetic domain wall with a head-to-head magnetization configuration.

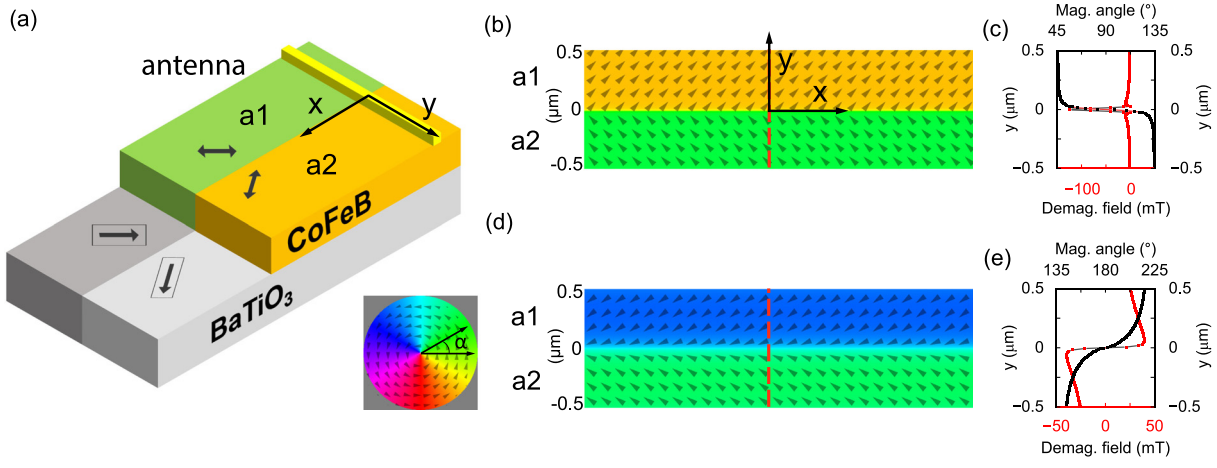

FIG. 1. (a) Schematic of the ferromagnetic/ferroelectric bilayer system with a field-programmable pinned magnetic domain wall and a microwave antenna. Strain coupling between the 90° polarization domains in the ferroelectric layer and the ferromagnetic film produces a fully correlated domain pattern with a_1 and a_2 domains. The domains exhibit uniaxial magnetic anisotropy, and the easy axis of magnetization rotates by 90° at the domain boundary. The abrupt change of magnetic anisotropy strongly pins the magnetic domain wall. In the simulations, we assume experimentally derived parameters from a CoFeB/$BaTiO_3$ bilayer. (b) Simulated remanent magnetization distribution for a head-to-tail magnetic domain wall. (c) Magnetization angle with respect to the x axis and demagnetizing field along the y axis extracted along the dashed line in (b). (d) Simulated remanent magnetization distribution for a head-to-head magnetic domain wall. (e) Magnetization angle with respect to the x axis and demagnetizing field along the y axis extracted along the dashed line in (d). The color wheel illustrates the direction of magnetization in the micromagnetic simulations in (b) and (d).

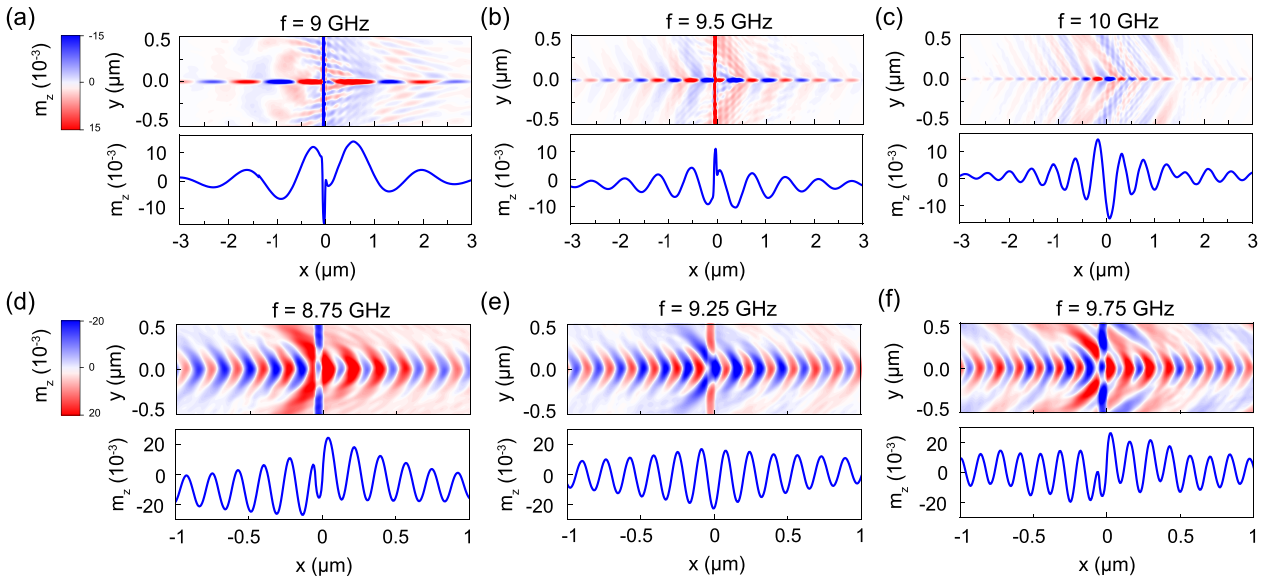

FIG. 2. (a)–(c) Simulated spatial maps and line profiles of propagating spin waves in a 90° head-to-tail domain wall at (a) 9, (b) 9.5, and (c) 10 GHz. (d)–(f) The same data for propagating spin waves in a 90° head-to-head domain wall at (d) 8.75, (e) 9.25, and (f) 9.75 GHz. All simulations are performed at zero magnetic field.

This domain wall is much broader than the head-to-tail wall, and the demagnetizing field within the domains changes sign. The magnetization in the wall center is oriented along the x axis rather than the y axis, and therefore, the dispersion of spin waves propagating along this wall is different.

Figures 2(a)–2(c) show simulated spatial maps and line profiles of propagating spin waves in the 90° head-to-tail domain wall at 9, 9.5, and 10 GHz. No external magnetic field is used in these simulations. Spin waves are excited at $x = 0\,\mu$m, and they propagate along the domain wall in the positive and negative x direction. The transport of spin waves at the selected frequencies is localized because the FMR frequency of the a_1 and a_2 domains is around 11 GHz. The microwave antenna does, therefore, not directly excite spin waves in the magnetic domains. The spin waves propagate perpendicular to the magnetization direction in the domain-wall center. The width of the head-to-tail wall is 36 nm, providing strong nanoscopic confinement. As the excitation frequency increases from 9 to 10 GHz, the wavelength of the spin waves decreases from 1.5 to 0.5 μm. Fitting the line profile in the lower panels of Figs. 2(a)–2(c) to $y = A\exp(-x/l_d)\sin(2\pi x/\lambda + \phi)$ gives a spin-wave decay length (l_d) of 1.32 and 1.01 μm at 9 and 10 GHz, respectively. The short decay length is caused by strong magnetic damping in the CoFeB film. The spin waves propagating along the domain wall excite low-intensity waves inside the magnetic domains [Figs. 2(a)–2(c)]. The intensity of these waves decreases away from the microwave antenna. The emitted spin waves from neighboring domain walls interfere within the domains. Figures 2(d)–2(f) show simulated spatial maps and line profiles of propagating spin waves in the 90° head-to-head domain wall. Now, the spin waves are confined to a much broader transporting channel as the head-to-head wall is about 1.43 μm wide. Moreover, the spin waves propagate parallel to the direction of magnetization at the domain wall center. Consequently, the wavelength of these spin waves is smaller at equal frequency. As the frequency increases from 8.25 to 9.75 GHz, the wavelength of the spin waves decreases from 174 to 136 nm. The spin-wave wavefront inside the broad head-to-head domain wall is curved because of a gradual rotation of magnetization.

Figure 3 shows the spin-wave dispersion for the two domain walls extracted from the data in Fig. 2 and simulations conducted at other frequencies. We note that switching between longer spin waves and shorter spin waves at the same frequency is implemented easily by resetting the spin structure of the pinned domain wall using an external magnetic field, as previously demonstrated in experiments.[28] For instance, a positive field pulse along the y axis initializes a head-to-tail domain wall, while a field pulse along the x axis stabilizes a head-to-head or tail-to-tail domain wall depending on the field direction. Reprogramming of the spin-wave mode in the domain-wall transporting channel is a unique feature of pinned magnetic domain walls in a strain-coupled multiferroic system with 90° rotations of uniaxial

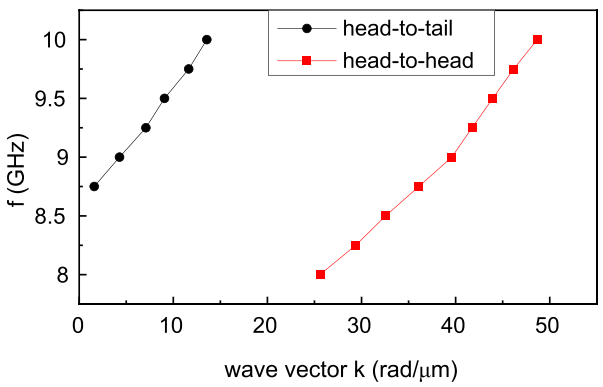

FIG. 3. Spin-wave dispersion for a head-to-tail domain wall (black circles) and a head-to-head domain wall (red squares) at zero magnetic field.

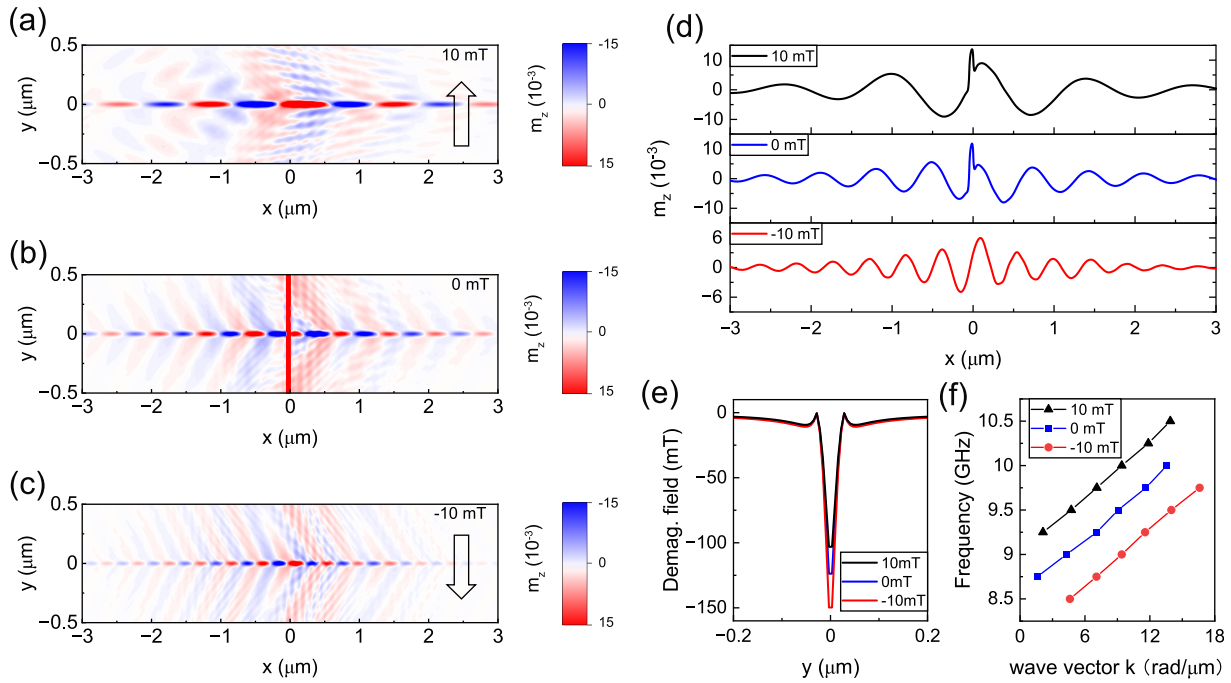

FIG. 4. (a)–(d) Simulated spatial maps and line profiles of propagating spin waves in a head-to-tail domain wall for an applied magnetic field of +10, 0, and −10 mT along the *y* axis. The excitation frequency is 9.5 GHz. (e) Demagnetizing field along the *y* axis for an applied magnetic field of +10, 0, and −10 mT. (f) Spin-wave dispersion for the head-to-tail domain wall at +10, 0, and −10 mT.

magnetic anisotropy. In addition to the toggling between two propagating modes, it is also possible to tune the properties of each mode continuously by an external magnetic field. We illustrate this for the head-to-tail domain wall and a magnetic field applied along the *y* axis, i.e., perpendicular to the domain wall. Figure 4 shows simulated spatial maps and line profiles of propagating spin waves in the head-to-tail domain wall for a magnetic field of +10, 0, and −10 mT. The excitation frequency is 9.5 GHz. The magnetic domain wall does not move under the action of an applied magnetic field because of strong pinning by the strain-induced rotation of uniaxial magnetic anisotropy.[23] Instead of domain wall motion, the external magnetic field rotates the magnetization in the a_1 and a_2 domains. For a +10 mT field, the spin rotation inside the domain wall decreases from 90° to 81°, whereas a −10 mT field increases the rotation of magnetization from 90° to 99°. The change in the spin rotation has a two-pronged effect. First, it alters the domain wall width and, thus, the localization of spin-wave transport. For +10, 0, and −10 mT, we find a head-to-tail domain wall width of 31, 36, and 44 nm, respectively. Second, field-induced tuning of the magnetization rotation modifies the wavelength of the spin waves propagating along the wall [Figs. 4(a)–4(d)] because of a changing demagnetizing field inside the wall [Fig. 4(e)]. Figure 4(f) summarizes the spin-wave dispersion of the head-to-tail domain wall for the three magnetic bias fields. Local reprogramming of the spin-wave wavelength by a small bias field could be utilized to control their phase in domain-wall circuits.

The pinning of magnetic domain walls onto ferroelectric domain walls in strain-coupled multiferroic systems allows for the driving of magnetic domain walls by an electric field.[24,25] In experiments, the reversible motion of magnetic domain walls by positive and negative voltages has been demonstrated for ferroelectric layers with alternating in-plane and out-of-plane polarization.[25,29] In this configuration, the application of a voltage perpendicular to the ferroelectric layer drives the pinned ferroelectric and magnetic domain walls in unison. Attaining a similar effect in the bilayer system considered here would require an in-plane electric field along the polarization direction of one of the *a* domains, which is more challenging but not impossible. In both multiferroic systems, the magnetic domain walls are strongly pinned onto the ferroelectric domain walls, providing versatile magnetic-field tuning of guided spin waves and electric-field control over the position of spin-wave nanochannels. The separation of mode control and routing could pave the way for realizing low-power magnonic circuits based on reconfigurable magnetic domain walls.

In summary, we investigated the use of pinned magnetic domain walls in a strain-coupled multiferroic heterostructure as programmable nanochannels for spin-wave transport. Micromagnetic simulations show localized spin-wave transmission along pinned domain walls below the FMR frequency of the magnetic domains. We demonstrate that an external magnetic field can be used to abruptly switch the propagating spin-wave mode or to continuously tune the wavelength of localized spin waves. Together with the potential to voltage control the position of magnetic domain walls, the studied systems offer unique features for reconfigurable magnonic devices.

This work has received funding from the European Union's Horizon 2020 research and innovation programme BeMAGIC under the Marie Sklodowska-Curie Grant Agreement No. 861145.

The work was supported also by the Academy of Finland (Grant Nos. 317918 and 325480). Computational resources were provided by the Aalto Science-IT project.

AUTHOR DECLARATIONS

Conflict of Interest

The authors have no conflicts to disclose.

Author Contributions

Weijia Zhu: Conceptualization (equal); Investigation (lead); Methodology (equal); Validation (equal); Visualization (equal); Writing – original draft (equal). **Huajun Qin:** Conceptualization (equal); Funding acquisition (lead); Investigation (equal); Methodology (equal); Project administration (equal); Resources (lead); Supervision (equal); Validation (equal); Visualization (equal); Writing – original draft (equal); Writing – review & editing (equal). **Sebastiaan van Dijken:** Conceptualization (equal); Funding acquisition (lead); Investigation (supporting); Project administration (equal); Resources (lead); Supervision (equal); Validation (equal); Writing – original draft (equal); Writing – review & editing (equal).

DATA AVAILABILITY

The data that support the findings of this study are available from the corresponding authors upon reasonable request.

REFERENCES

[1]A. Khitun, M. Bao, and K. L. Wang, "Magnonic logic circuits," J. Phys. D **43**, 264005 (2010).
[2]V. V. Kruglyak, S. O. Demokritov, and D. Grundler, "Magnonics," J. Phys. D **43**, 264001 (2010).
[3]B. Lenk, H. Ulrichs, F. Garbs, and M. Münzenberg, "The building blocks of magnonics," Phys. Rep. **507**, 107–136 (2011).
[4]A. V. Chumak, V. I. Vasyuchka, A. A. Serga, and B. Hillebrands, "Magnon spintronics," Nat. Phys. **11**, 453–461 (2015).
[5]A. Barman, G. Gubbiotti, S. Ladak *et al.*, "The 2021 magnonics roadmap," J. Phys.: Condens. Matter **33**, 413001 (2021).
[6]A. Chumak, P. Kabos, M. Wu *et al.*, "Advances in magnetics roadmap on spin-wave computing," IEEE Trans. Magn. **58**, 0800172 (2022).
[7]K. Wagner, A. Kákay, K. Schultheiss, A. Henschke, T. Sebastian, and H. Schultheiss, "Magnetic domain walls as reconfigurable spin-wave nanochannels," Nat. Nanotechnol. **11**, 432–436 (2016).
[8]V. Sluka, T. Schneider, R. A. Gallardo, A. Kákay, M. Weigand, T. Warnatz, R. Mattheis, A. Roldán-Molina, P. Landeros, V. Tiberkevich, A. Slavin, G. Schütz, A. Erbe, A. Deac, J. Lindner, J. Raabe, J. Fassbender, and S. Wintz, "Emission and propagation of 1D and 2D spin waves with nanoscale wavelengths in anisotropic spin textures," Nat. Nanotechnol. **14**, 328–333 (2019).
[9]L.-J. Chang, J. Chen, D. Qu, L.-Z. Tsai, Y.-F. Liu, M.-Y. Kao, J.-Z. Liang, T.-S. Wu, T.-M. Chuang, H. Yu, and S.-F. Lee, "Spin wave injection and propagation in a magnetic nanochannel from a vortex core," Nano Lett. **20**, 3140–3146 (2020).
[10]E. Albisetti, D. Petti, G. Sala, R. Silvani, S. Tacchi, S. Finizio, S. Wintz, A. Calò, X. Zheng, J. Raabe, E. Riedo, and R. Bertacco, "Nanoscale spin-wave circuits based on engineered reconfigurable spin-textures," Commun. Phys. **1**, 56 (2018).
[11]B. Mozooni and J. McCord, "Direct observation of closure domain wall mediated spin waves," Appl. Phys. Lett. **107**, 042402 (2015).
[12]J. Trützschler, K. Sentosun, B. Mozooni, R. Mattheis, and J. McCord, "Magnetic domain wall gratings for magnetization reversal tuning and confined dynamic mode localization," Sci. Rep. **6**, 30761 (2016).
[13]F. Garcia-Sanchez, P. Borys, R. Soucaille, J.-P. Adam, R. L. Stamps, and J.-V. Kim, "Narrow magnonic waveguides based on domain walls," Phys. Rev. Lett. **114**, 247206 (2015).
[14]J. Lan, W. Yu, R. Wu, and J. Xiao, "Spin-wave diode," Phys. Rev. X **5**, 041049 (2015).
[15]Y. Henry, D. Stoeffler, J.-V. Kim, and M. Bailleul, "Unidirectional spin-wave channeling along magnetic domain walls of Bloch type," Phys. Rev. B **100**, 024416 (2019).
[16]J. Chen, J. Hu, and H. Yu, "Chiral magnonics: Reprogrammable nanoscale spin wave networks based on chiral domain walls," iScience **23**, 101153 (2020).
[17]X. Liang, Z. Wang, P. Yan, and Y. Zhou, "Nonreciprocal spin waves in ferrimagnetic domain-wall channels," Phys. Rev. B **106**, 224413 (2022).
[18]H.-K. Park and S.-K. Kim, "Channeling of spin waves in antiferromagnetic domain walls," Phys. Rev. B **103**, 214420 (2021).
[19]L. Qiu and K. Shen, "Tunable spin-wave nonreciprocity in synthetic antiferromagnetic domain walls," Phys. Rev. B **105**, 094436 (2022).
[20]M. Zhao, X.-G. Wang, Z. Luo, Q.-L. Xia, Y.-Z. Nie, R. Xiong, and G.-H. Guo, "Reconfigurable spin-wave coupler based on domain-wall channels," Phys. Rev. Appl. **17**, 064013 (2022).
[21]J. M. Winter, "Bloch wall excitation. Application to nuclear resonance in a Bloch wall," Phys. Rev. **124**, 452–459 (1961).
[22]T. Taniyama, "Electric-field control of magnetism via strain transfer across ferromagnetic/ferroelectric interfaces," J. Phys.: Condens. Matter **27**, 504001 (2015).
[23]K. J. A. Franke, T. H. E. Lahtinen, and S. van Dijken, "Field tuning of ferromagnetic domain walls on elastically coupled ferroelectric domain boundaries," Phys. Rev. B **85**, 094423 (2012).
[24]T. H. E. Lahtinen, K. J. A. Franke, and S. van Dijken, "Electric-field control of magnetic domain wall motion and local magnetization reversal," Sci. Rep. **2**, 258 (2012).
[25]K. J. A. Franke, B. Van de Wiele, Y. Shirahata, S. J. Hämäläinen, T. Taniyama, and S. van Dijken, "Reversible electric-field-driven magnetic domain-wall motion," Phys. Rev. X **5**, 011010 (2015).
[26]B. Van de Wiele, S. J. Hämäläinen, P. Baláž, F. Montoncello, and S. van Dijken, "Tunable short-wavelength spin wave excitation from pinned magnetic domain walls," Sci. Rep. **6**, 21330 (2016).
[27]S. J. Hämäläinen, F. Brandl, K. J. A. Franke, D. Grundler, and S. van Dijken, "Tunable short-wavelength spin-wave emission and confinement in anisotropy-modulated multiferroic heterostructures," Phys. Rev. Appl. **8**, 014020 (2017).
[28]S. J. Hämäläinen, M. Madami, H. Qin, G. Gubbiotti, and S. van Dijken, "Control of spin-wave transmission by a programmable domain wall," Nat. Commun. **9**, 4853 (2018).
[29]H. Qin, R. Dreyer, G. Woltersdorf, T. Taniyama, and S. van Dijken, "Electric-field control of propagating spin waves by ferroelectric domain-wall motion in a multiferroic heterostructure," Adv. Mater. **33**, 2100646 (2021).
[30]T. H. E. Lahtinen, J. O. Tuomi, and S. van Dijken, "Pattern transfer and electric-field-induced magnetic domain formation in multiferroic heterostructures," Adv. Mater. **23**, 3187–3191 (2011).
[31]A. Vansteenkiste, J. Leliaert, M. Dvornik, M. Helsen, F. Garcia-Sanchez, and B. Van Waeyenberge, "The design and verification of MuMax3," AIP Adv. **4**, 107133 (2014).